JOURNAL OF GEOPHYSICAL RESEARCH, VOL. 104, NO. D24, PAGES 30,937–30,946, DECEMBER 27, 1999

Propagation of the Arctic Oscillation from the stratosphere to the troposphere

Mark P. Baldwin and Timothy J. Dunkerton

Northwest Research Associates, Bellevue, Washington

Abstract. Geopotential anomalies ranging from the Earth's surface to the middle stratosphere in the northern hemisphere are dominated by a mode of variability known as the Arctic Oscillation (AO). The AO is represented herein by the leading mode (the first empirical orthogonal function) of low-frequency variability of wintertime geopotential between 1000 and 10 hPa. In the middle stratosphere the signature of the AO is a nearly zonally symmetric pattern representing a strong or weak polar vortex. At 1000 hPa the AO is similar to the North Atlantic Oscillation, but with more zonal symmetry, especially at high latitudes. In zonal-mean zonal wind the AO is seen as a north-south dipole centered on 40°–45°N; in zonal-mean temperature it is seen as a deep warm or cold polar anomaly from the upper troposphere to ~10 hPa. The association of the AO pattern in the troposphere with modulation of the strength of the stratospheric polar vortex provides perhaps the best measure of coupling between the stratosphere and the troposphere. By examining separately time series of AO signatures at tropospheric and stratospheric levels, it is shown that AO anomalies typically appear first in the stratosphere and propagate downward. The midwinter correlation between the 90-day low-pass-filtered 10-hPa anomaly and the 1000-hPa anomaly exceeds 0.65 when the surface anomaly time series is lagged by about three weeks. The tropospheric signature of the AO anomaly is characterized by substantial changes to the storm tracks and strength of the midtropospheric flow, especially over the North Atlantic and Europe. The implications of large stratospheric anomalies as precursors to changes in tropospheric weather patterns are discussed.

1. Introduction

A coupled mode of variability between the northern winter stratosphere and troposphere was discussed by *Nigam* [1990], who examined rotated empirical orthogonal functions (EOFs) of zonal-mean wind. Nigam's result showed that the dominant mode of variability in zonal-mean wind appears as a deep north-south dipole, with a node near 40°–45°N. The poleward part of the dipole represents fluctuations in the strength of the polar vortex. Coupling between the stratosphere and troposphere was further explored by *Baldwin et al.* [1994], who examined geopotential patterns in the middle troposphere that were linked to the stratosphere. By using singular value decomposition (SVD, *Bretherton et al.*, [1992]) between 500- and 50-hPa geopotential, they showed that the leading mode had a strong dipole signature in zonal-mean wind, extending from the surface to above 10 hPa. They found that the dominant 500-hPa pattern was a mode similar to the North Atlantic Oscillation (NAO), with centers of action near Greenland and just west of Spain, but with a slightly larger spatial extent than the NAO and a large degree of circular symmetry about a center point displaced toward Greenland. They suggested that elements of this pattern may act to force the stratosphere but also that part of the tropospheric pattern may represent downward influence from the stratosphere.

Thompson and Wallace [1998] examined the leading EOF of northern winter sea-level pressure (SLP) and found a wintertime pattern resembling the NAO, but with the primary center of action covering more of the Arctic, giving a more zonally symmetric appearance. They called the leading EOF of SLP the Arctic Oscillation (AO). The AO is remarkably similar to the spatial pattern produced by using the original definition of the NAO [*Walker and Bliss*, 1932]. The NAO index was first defined as a linear combination of normalized pressures and temperatures from nine stations covering 90° of longitude from Washington, DC to Vienna. The resulting spatial pattern is substantially more strongly correlated with the AO index than with "Atlanti-centric" indices such as the normalized SLP difference between Portugal and Iceland (J.M. Wallace, University of Washington, personal communication). Nevertheless, a comparison of the NAO (as illustrated in *Hurrell* [1995]) with the AO shows a nearly identical pattern in middle to high latitudes from North America to Europe. The main differences are 1) the NAO has no center of action in the Pacific, and 2) the AO has a more broad center of action over the polar cap. The close match between the AO and NAO across the Atlantic region imply that the weather and climate implications of the AO will be similar to that of the NAO.

Even though the AO was defined on the basis of surface data, it showed remarkably strong coupling to the stratosphere. Thompson and Wallace also showed the 500-hPa and

Paper Number 1999JD900445.
0148-0227/99/1999JD900445$09.00

50-hPa signatures of the AO (regressions of their AO index with geopotential fields). A comparison (at 500 and 50 hPa) with the leading SVD mode of *Baldwin et al.* [1994] shows that the two modes are nearly identical. SVD analysis between 500 and 50 hPa captures the same mode of variability as does EOF analysis of surface pressure. The AO represents a dominant, robust, naturally occurring mode of variability, which may be recovered by using tropospheric data or a combination of tropospheric and stratospheric data. The AO is also seen in stratosphere-troposphere general circulation models, and its trend reveals a possible link to greenhouse gas increases [*Shindell et al.*, 1999]. For a brief overview of the AO and climate connections, see *Kerr* [1999].

Downward propagation of stratospheric disturbances into the troposphere has been observed in data and simulated in general circulation models. Stratospheric sudden warmings often begin in the lower mesosphere (~60 km) and develop downward, and case studies of warmings have documented penetration to the Earth's surface. *Kodera et al.* [1990] observed that strong upper-stratospheric westerlies in December tend to propagate poleward and downward, so that tropospheric westerlies at high latitudes are stronger during the following February. This behavior was also simulated in a general circulation model. Kodera and Koide [1997] discussed the formation of an AO-like circulation in the troposphere in association with the downward propagation of zonal wind anomalies from the stratosphere.

We take the view that the AO is the largest and most fundamental mode of variability in the northern hemisphere troposphere-stratosphere system. During winter, when the stratosphere has large-amplitude disturbances, the AO has a strong signature in the stratosphere. Outside of winter the AO is confined to the troposphere, although with greatly diminished amplitude (~⅓) during summer.

Section 5 is a glossary of terms. Each term is italicized when first used.

2. Data Set and Analysis Technique

We use the National Centers for Environmental Prediction/National Center for Atmospheric Research (NCEP/NCAR) Reanalysis [*Kalnay et al.*, 1996]. These geopotential, wind, and temperature data are global and are archived as daily averages on a 2.5° × 2.5° grid and are available at 17 levels from 1000 to 10 hPa for the period 1958–1997.

Our approach differs somewhat from either *Baldwin et al.* [1994] or *Thompson and Wallace* [1998]; we examine the leading EOF of a deep layer of the wintertime stratosphere-troposphere, represented by the five geopotential fields at 1000, 300, 100, 30 and 10 hPa, using 90-day low-pass-filtered data north of 20°N. The data at each of the five levels were normalized by dividing by the spatial standard deviation at each level. As noted by *Thompson and Wallace* [1998], energy density of the AO (the product of density and squared amplitude) will be roughly invariant over the five data levels, which argues for equal weighting of each level. In practice, the details of the weighting are unimportant; Thompson and Wallace obtained a similar leading mode with monthly-mean surface data. We confine the EOF analysis to wintertime (December–February) so that stratospheric winds tend to be westerly, allowing upward propagation of large-scale tropospheric waves [*Charney and Drazin*, 1961]. (We also tried including November and March with little effect on the results.) We treat the five levels of geopotential as a single field for the purpose of the EOF calculation. Each NCEP latitude-longitude grid was resampled onto an equal-area grid. The AO pattern was identified as the leading EOF of the temporal covariance matrix of the five-level geopotential data. The *AO index* is defined as the daily time series of the first mode (often called the principal component time series) based on the 90-day low-pass-filtered geopotential data. We then show the spatial patterns of the AO by regressing the AO index with various 90-day low-pass filtered data fields; we call the resulting patterns the *signatures of the AO*. As noted by *Thompson and Wallace* [1999], the regression maps are not precisely the same as the EOFs because of the weightings used in the calculation. The regression maps correspond to anomaly values in a field associated with a one standard deviation fluctuation in the nondimensional AO index.

3. Results

3.1. Signatures of Arctic Oscillation

The Arctic Oscillation accounts for 23% of the variance in the five-level data set (as compared with 22% in Thompson and Wallace's [1998] SLP AO). Figure 1 illustrates the signatures of the leading mode at nine levels, including the five levels used to define the AO. The panels are contoured in meters per standard deviation of AO index. We now compare the 1000-, 500-, and 50-hPa panels in Figure 1 with the corresponding panels in Figure 1 of *Thompson and Wallace* [1998]. The 1000-hPa panel is nearly identical to Thompson and Wallace's SLP AO regression. This mode has been discussed by several authors beginning, with *Kutzbach* [1970], and is characterized by one center of action over the Arctic region, displaced toward Greenland, and an opposing ring at midlatitudes with prominent features over both the Atlantic and Pacific Oceans. The Atlantic region resembles the NAO, but the pattern is more zonally symmetric and has a larger spatial scale. The agreement is remarkable considering that Thompson and Wallace used monthly-mean November–April data only at 1000 hPa, and we use 90-day low-pass-filtered December–February data spanning 1000–10 hPa.

The 500-hPa panel again captures the same mode as Thompson and Wallace [1998], with one center of action over southern Greenland opposing a broad midlatitude band. Figure 3a from *Baldwin et al.* [1994] illustrates that the 500-hPa pattern resulting from SVD between 50 and 500-hPa is essentially similar to that shown in Figure 1 or that shown by Thompson and Wallace. In the stratosphere the 50-hPa pattern is dominated by a center of action displaced slightly off the pole toward Greenland, with a nearly zonally symmetric ring in midlatitudes. As with the 500-hPa pattern, the 50-hPa pattern is nearly the same as either the SVD mode of *Baldwin et al.* [1994] or the AO signature of *Thompson and Wallace* [1998]. The 10-hPa panel shows a pattern centered nearly over the pole, but with less zonal symmetry in midlatitudes, featuring an opposing center of action over the eastern Pacific.

The above comparisons show that the AO is extraordinarily robust, in that it may be recovered using a variety of data levels and techniques, and it is not sensitive to the number of months included in the winter season. Other than the seasonal cycle, the AO is the largest mode of variability in the extratropical northern troposphere-stratosphere.

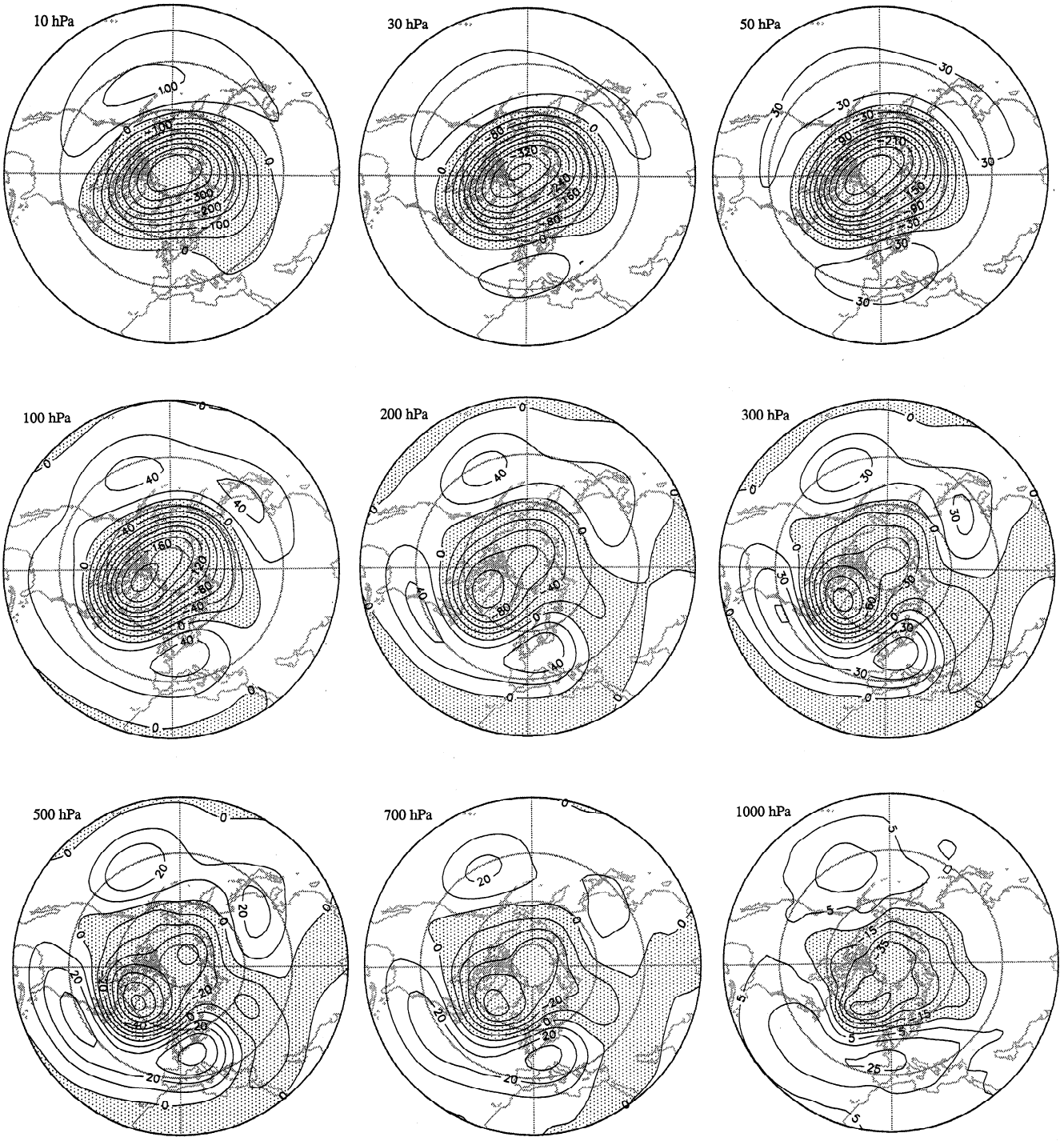

Figure 1. Signatures of the Arctic Oscillation (AO) at 10, 30, 50, 100, 200, 300, 500, 700, and 1000 hPa. Each panel is produced by regressing the AO index with geopotential. Contour values are meters, corresponding to a one standard deviation anomaly in the AO index. The contour interval of the 1000-hPa panel is ±5, ±15,... for ease of comparison with *Thompson and Wallace* [1998].

Figure 2a illustrates correlations between the AO index and zonal-mean wind. The AO accounts for 34% of the variance in the region north of 20°N. The dipole structure is similar to that illustrated by *Baldwin et al.* [1994] for SVD between 500- and 50-hPa height fields and has correlations up to 0.96 at 60°N, 100 hPa. *Kodera et al.* [1999] defined the "polar night jet (PNJ) index" as the zonal-mean wind at 65°N and 50 hPa, which is also highly correlated (0.93) with the AO index. The regression of the AO index with zonal-mean wind (Figure 2b) shows that the wind oscillation exceeds 10 m s^{-1} in the middle stratosphere. If the same calculation is performed for angular momentum, the northern and southern parts of the dipole are very similar in magnitude.

Correlations between the AO index and zonal-mean tem-

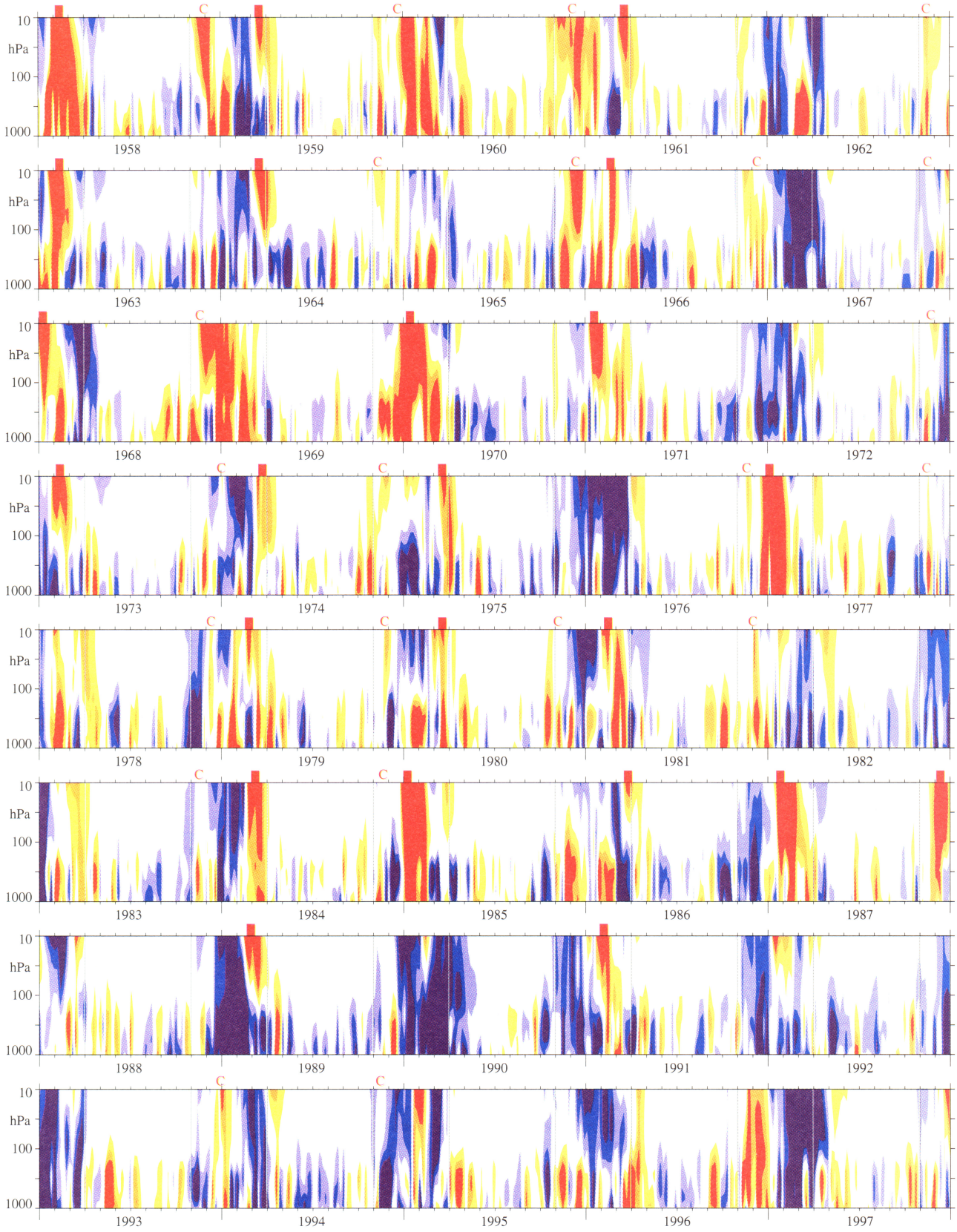

Plate 1. The 10-day low-pass filtered AO signature time series for 1958-1997. Contours are ±0.5, ±1.0, ±1.5, with values between -0.5 and 0.5 not shaded. Red corresponds to a weak, warm polar vortex, while blue indicates a strong, cold vortex. Vertical lines denote the November–March winter season. Red ticks indicate major midwinter or early final warmings during December–March. Each red "C" indicates a Canadian warming.

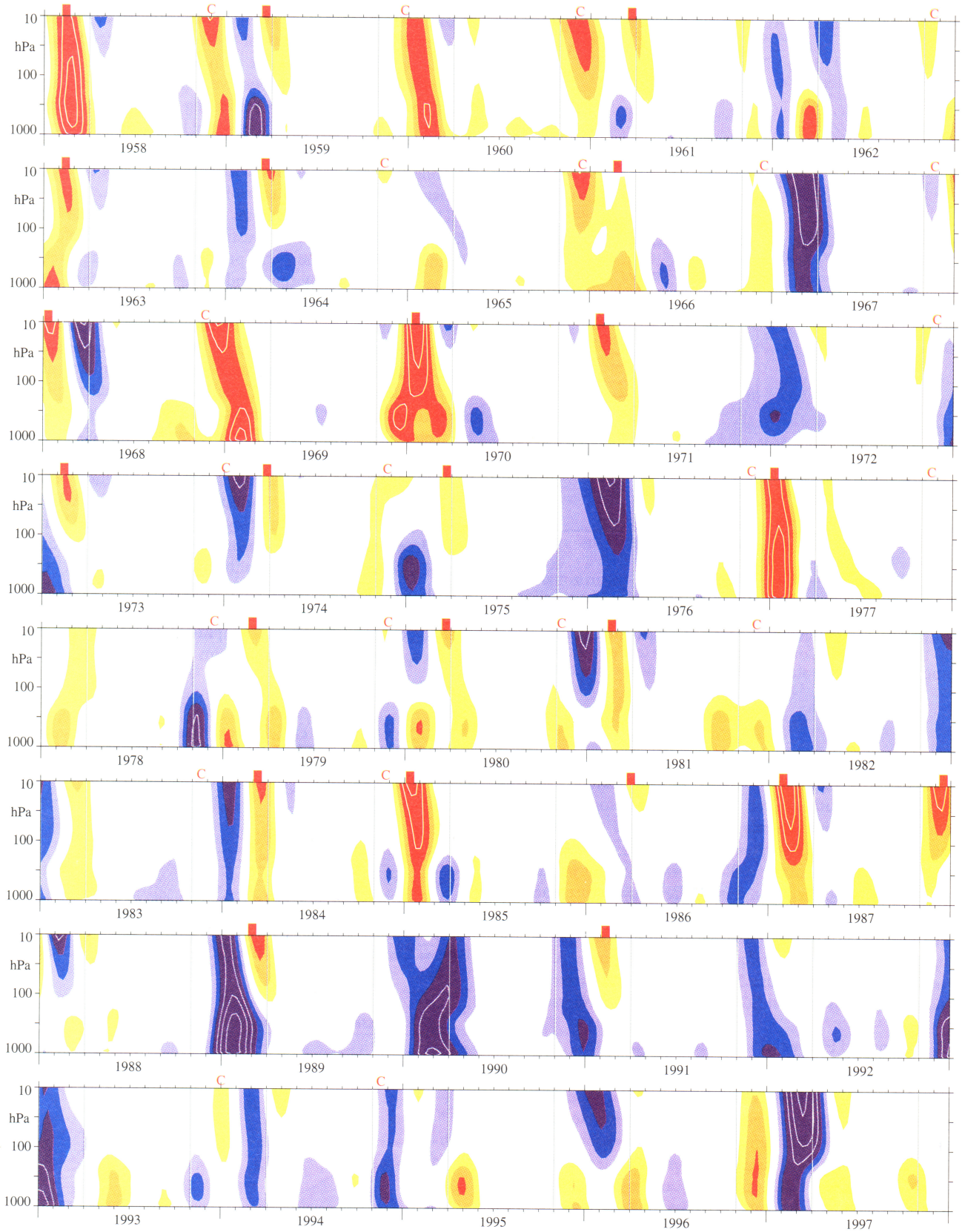

Plate 2. The 90-day low-pass-filtered AO signature time series for 1958-1997. Shaded contour values are ±0.5, ±1.0, ±1.5, with white contours indicating ±2.0, ±2.5,... Values between -0.5 and 0.5 are not shaded. Red corresponds to a weak, warm polar vortex, while blue indicates a strong, cold vortex. Vertical lines denote the November–March winter season. Red ticks indicate major midwinter or early final warmings during December–March. Each red "C" indicates that a warm AO event corresponds to a Canadian warming.

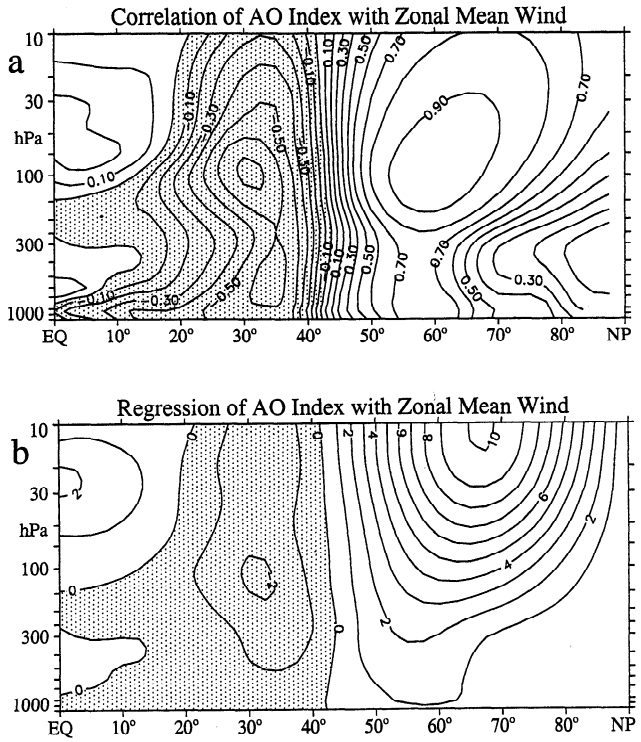

Figure 2. (a) Correlations between zonal-mean zonal wind and the AO index during December–February. The minimum correlation is -0.72, and the maximum is 0.96. (b) Same as Figure 2a, except regression between zonal-mean zonal wind and the AO index. Contour values are meters per second, corresponding to a one standard deviation anomaly in the AO index.

perature (Figure 3a) exceed 0.90 at 150 hPa and 80°N. The AO accounts for 22% of the variance in temperature north of 20°N. In the southern half of the dipole, correlations are strong near the midlatitude tropopause and extend to the equator. Figure 3b illustrates the regression between zonal-mean temperature and the AO time series and shows that the AO could be described as a deep polar temperature anomaly extending from the upper troposphere to the middle stratosphere, with a compensating anomaly south of ~50°N. In the tropics the anomaly is confined to the stratosphere. A pattern essentially similar to Figure 3b was shown in *Dunkerton and Baldwin* [1992] as the first EOF of zonal-mean temperature.

3.2. Downward Propagation of the AO Signature

The above analysis of the AO describes a spatially fixed pattern and does not allow for the analysis of vertical development of the AO or suggest cause and effect. However, the regressions result in different signatures (maps) for each of the 17 pressure levels. These signature maps characterize the AO at each level, and the signature maps can be compared to the daily anomalies in the data to measure how close a daily anomaly map is to the pattern representing the AO. If $Z10_{AO}$ is the 10-hPa signature of the AO, and $Z10$ is a daily map of deseasoned 10 hPa Z, then

$$\min \left| Z10 - \alpha Z10_{AO} \right|^2$$

defines α as the multiple of $Z10_{AO}$ that results in a "best fit" of the AO signature to the daily map. This calculation was performed for every day of the 40-year data set at each level, yielding a 17 × 14609 array of the daily AO α coefficients at each level. The time series at each level represents the daily values of the AO signature (positive, corresponding to a strong polar vortex, or negative, representing a weak vortex) and is calculated independently of the other levels. The resulting array, which we call the *AO signature time series*, may be used to examine whether AO signals tend to appear at the surface and propagate upward to the stratosphere or vice versa.

The AO signature time series was used to calculate the *climatological AO amplitude*, illustrated in Figure 4. Before the original EOF calculation was performed, the data were normalized by dividing by the standard deviation of the December–February 90-day low-pass geopotential fields. Thus the AO signature time series is nondimensional at each level. Contours show the climatological AO amplitude, defined as the rms value of the AO signature time series for each day of the year and each data level. The climatological AO amplitude peaks near February 1 at all levels. The relatively large values in the troposphere and near 10 hPa indicate that the AO accounts for a larger fraction of the spatial variance there than at levels in the lower stratosphere. There is a clear distinction between the behavior of the AO in the troposphere and the AO in the stratosphere, with the climatological stratospheric AO amplitude dropping rapidly in spring to very low levels during June–October. Large AO amplitudes are found when stratospheric winds are westerly, allowing the upward propagation of planetary waves from the troposphere. In contrast, the climatological tropospheric AO amplitude diminishes gradually in the spring, reaching a minimum of ~⅓ of its wintertime

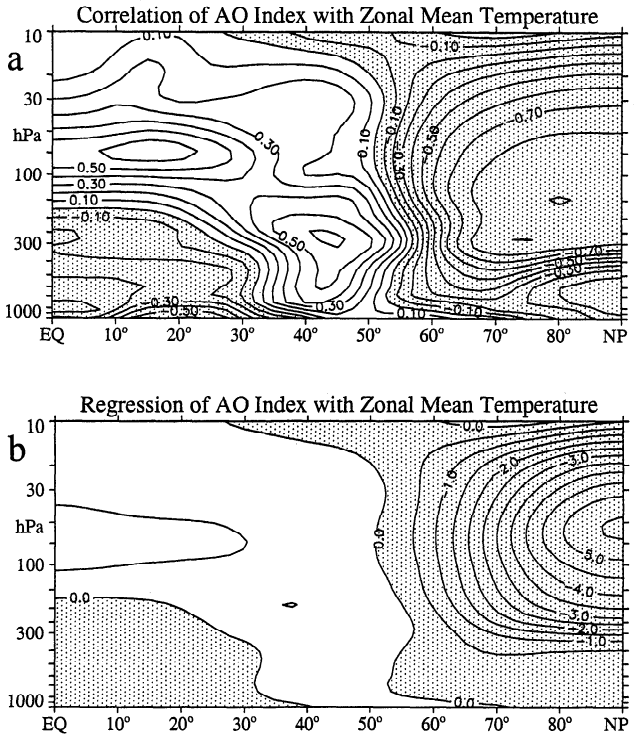

Figure 3. (a) Correlations between zonal-mean temperature and the AO index during December–February. The minimum correlation is -0.90 and the maximum is 0.65. (b) Same as Figure 3a, except regression between zonal-mean temperature and the AO index. Contour values are kelvins, corresponding to a one standard deviation anomaly in the AO index.

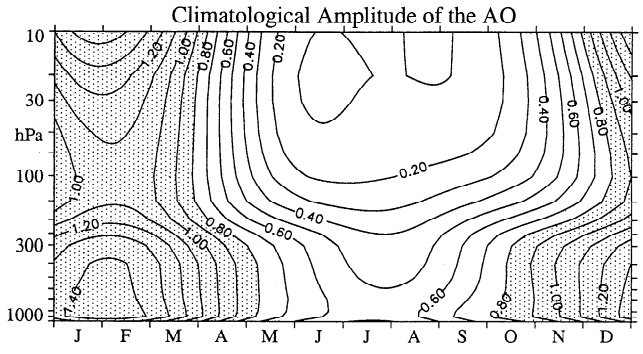

Figure 4. Climatological amplitude of the Arctic Oscillation. The contoured values are the rms values of the AO signature time series.

peak amplitude, before beginning to increase in September. This behavior is seen clearly in a comparison of the variability of 1000-hPa and 50-hPa geopotential over the polar cap [*Thompson and Wallace*, 1999].

The height-time development of AO signature time series, for 40 years of data, is illustrated in Plate 1. The data have been 10-day low-pass filtered to eliminate synoptic-scale events. Red shading corresponds to a weak polar vortex, as during a stratospheric warming, while blue shading indicates a strong, cold vortex. A value of 1.0 corresponds to the definition of the AO signature at each level (Figure 1). The contour interval is 0.5 with values between -0.5 and 0.5 not shaded, and values exceeding -1.5 and 1.5 in solid red or blue shading, respectively. Vertical gray lines define the November–March winter season. The large magnitudes of the AO are, in the stratosphere, confined almost entirely to the period October–April, while occasional large-amplitude events may be found in the troposphere at any time of the year, consistent with the climatology illustrated in figure 4. Many of the stratospheric events are connected to tropospheric events, but the connection is typically intermittent, involving fairly rapid vertical bursts which tend to descend farther into the troposphere over a period of several weeks (e.g. 1960–1961, 1968–1969, 1973–1974). In some cases, downward penetration of positive (red) AO anomalies occurred continuously over a period of ~2 weeks (e.g., 1958–1959, 1984–1985).

In the stratosphere, each winter has typically only one or two sustained large-amplitude anomalies, while the timescale in the troposphere appears much shorter. To isolate the low-frequency vertical propagation visible in Plate 1, the data were 90-day low-pass filtered. Above 150 hPa, 66% of the unfiltered variance is retained by the 90-day low-pass filter, while below 200 hPa, only 39% is retained. Plate 2 shows that many events (typically one or two per winter) are connected in the vertical from the middle stratosphere to the surface. The troposphere has events with large AO amplitudes which are not connected to the stratosphere, especially outside the winter season. Some stratospheric events do not reach the troposphere, but in most cases there is some penetration of the troposphere. Typically, the AO anomalies begin at 10 hPa or above and move downward over a period of a few weeks. The time delay is quite variable, ranging from near zero (e.g., December 1996) to more than a month (e.g., December 1968). This reflects the sporadic nature of the bursts of large AO magnitude. Only when low-pass filtered does the downward propagation appear smooth. Anomalies of both signs appear to propagate downward; there is no obvious preference for anomalies of either sign when the data are 90-day low-pass filtered. There is also a tendency for more rapid vertical propagation when the anomalies reach the troposphere (e.g., winters 1958–1959 and 1968–1969).

The AO events which correspond to a weak polar vortex show a remarkable correspondence to stratospheric sudden warmings. All major midwinter warmings and all final warmings during or before February are indicated in Plates 1 and 2 by red ticks at the top of each panel. The occurrences of warmings were defined [K. Labitzke, Frei University of Berlin, personal communication, 1998] on the basis of the synoptic situations and the standard definition of the World Meteorological Organization, which requires, at 10 hPa, easterly winds at 60°N and warmer temperatures at the pole than at 60°N. Although warmings appear to happen rapidly, there is typically a period before the warming during which the vortex is reduced in size (preconditioned). Recovery of the vortex after a warming is largely a radiative process and is relatively slow. The warmings are of large enough magnitude and their life cycle is long enough for these events to be seen clearly in 90-day low-pass-filtered data. In the stratosphere, sudden warmings cause the AO index to rapidly become negative, but a return to positive values is also relatively slow. (The warmings tend to occur rather abruptly at the beginning of the positive AO events, and the events are sometimes followed by lingering positive anomalies.) The skewness of the unfiltered 10-hPa AO signature time series is -0.70, while that of the 90-day low-pass time series is -0.07. The low-pass filter tends to make sudden warmings appear more symmetric in time.

Every major or early final warming during December–February (marked in Plates 2 and 3 by a wide red tick) corresponds to a large negative deviation in the AO signature time series. In addition, many, but not all, of the early winter events correspond to "Canadian warmings," marked by a red "C," during which the Aleutian high develops to disrupt and displace the vortex. If the vortex is displaced from the pole, but without diminution of the circulation, the signature in the AO magnitude time series is minimal.

The low-frequency vertical development of the AO was also investigated using a lag correlation technique. Figure 5 illustrates the correlation between the 90-day low-pass AO signature time series at 10 hPa on January 1 (the key date for the calculation) with the AO signature time series at all other levels during November–March. The dominant feature is strong downward propagation through the lower stratosphere into the troposphere, with lag correlations exceeding 0.65 at 1000

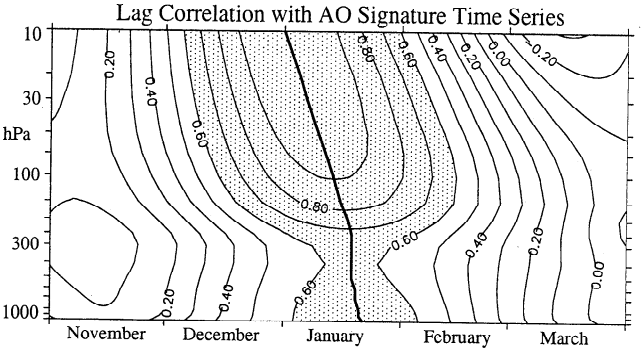

Figure 5. Correlations between the 90-day low-pass AO signature time series at 10 hPa on January 1 with the AO signature time series at all levels during November-March.

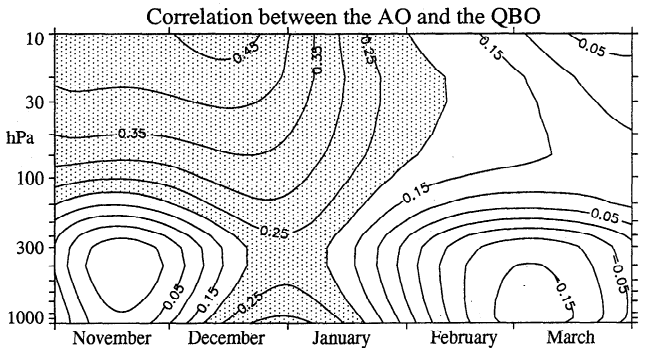

Figure 6. Correlation between the 40-hPa quasi-biennial oscillation (QBO) and the AO signature time series during November–March. The AO time series varies by day and level, while the QBO is defined by monthly-mean Singapore winds.

hPa ~3 weeks later. The thick line illustrates the peak correlation at each level. The lag correlations in figure 5 should not be interpreted to indicate a precise downward propagation speed; rather, they indicate an overall tendency for downward propagation on a timescale of a few weeks.

The downward propagation into the troposphere is confined to low-frequency variability. Lag correlations using higher frequencies (e.g., 90-day high-pass data) show little connection to the troposphere with the highest correlations found near zero lag, so that the tilt of the contours in Figure 5 is not present.

The same calculation as shown in Figure 5 was performed using key dates ranging from November 1 through March 1 (not shown). Both earlier and later dates resulted in slightly lower correlations in the troposphere but similar downward propagation. During early winter (November through early December) the contours in the stratosphere are more vertical, indicating more rapid vertical propagation. As winter progresses, the speed of downward propagation tends to be less, so that by March, the slope of the contours in the stratosphere tends to be slightly less vertical than seen in Figure 5.

3.3. Relation to the Quasi-Biennial Oscillation

The phase of the equatorial quasi-biennial oscillation (QBO), through modulation of the zonal-mean wind, affects the upward and equatorward propagation of planetary-scale waves. Warmings are more likely when the QBO is in its easterly phase, and Plates 1 and 2 show an excellent correspondence between the AO and sudden warmings. *Holton and Tan* [1980] examined northern hemisphere geopotential on the basis of the phase of the 50-hPa QBO and showed a stratospheric signature of the QBO that is similar to that of the AO. They also showed, using a 16-year data set, a 1000-hPa signature of the QBO during January that was similar to that of the AO. An update of that figure, using data for 1964–1996 (not shown), confirms that the pattern persists. Figure 2 shows that correlations between the AO amplitude and lower stratospheric equatorial zonal-mean wind are not zero, suggesting that the QBO may act to modulate the AO.

A time-height cross section of correlations between AO signature time series (for each day of year and level) and Singapore 40-hPa wind (which varies by month) is shown as Figure 6. Correlations peak above 0.45 at 10 hPa during December and fall off to less than 0.20 by February, indicating that any influence from the QBO appears to be confined to early winter. *Baldwin and Dunkerton* [1998] showed that the influence of the QBO on the zonal-mean wind is also an early winter phenomenon, with the largest influence in January and greatly diminished by February.

The signatures of the QBO and the AO are not the same—the QBO signature is more confined to the stratosphere and its influence on the high-latitude circulation is negligible after January. The correlations between the QBO and the AO are consistent with correlations between the QBO and zonal-mean

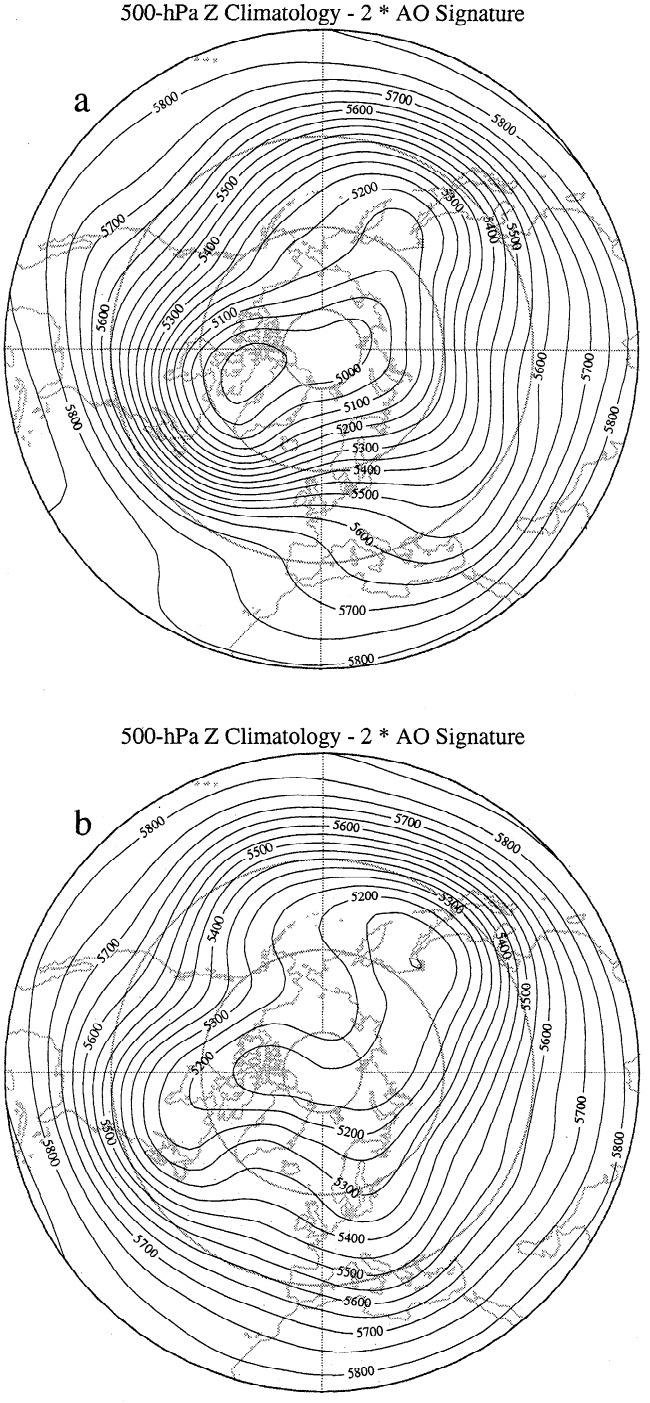

Figure 7. Extremes of the Arctic Oscillation at 500 hPa: (a) 500-hPa December–February climatology plus 2 × AO signature, and (b) 500-hPa December–February climatology minus 2 × AO signature.

zonal wind [*Baldwin and Dunkerton*, 1998], which show lower values below the tropopause. The QBO appears to be a factor that tends to excite the AO, but the influence is strongest in the stratosphere during early winter.

4. Discussion

The difference in tropospheric circulation patterns between the two extremes of the AO is considerable. In Figure 7a twice the 500-hPa AO anomaly is added to the climatological mean 500-hPa flow, while in Figure 7b twice the AO anomaly is subtracted from the climatology. The AO magnitude is observed to be this large at 500 hPa on ~3% of winter days. Since surface cyclones tend to be steered by the 500-hPa flow and typically move at ~½ the speed of the 500-hPa wind, these maps suggest dramatic difference in the location of storm tracks and surface cyclone activity between the two extremes of the AO. In the Atlantic sector the effects on weather will be similar to that of the NAO, as discussed in Hurrell [1995] and references therein. When the AO index is negative (Figure 7b), the flow over coastal Europe is weak and is from the west or west northwest. In contrast, when the AO index is positive, there is strong west southwesterly flow.

Large-amplitude stratospheric AO anomalies tend to precede large-amplitude tropospheric AO anomalies, which have an effect on storm tracks, the strength of tropospheric jets, and weather, especially over Europe. There are case studies and anecdotal evidence that sudden warmings precede certain weather patterns [e.g., *Quiroz*, 1986]. Stratospheric events are precursors to tropospheric events when the stratospheric AO amplitude is large and persistent. Long-range forecast models must have a realistic representation of stratospheric processes and planetary wave propagation if the downward propagation is to be forecast successfully. If climate models are to represent accurately the relationship between the stratosphere and the troposphere, such models should show not just the AO, but also downward propagation of the AO. Both downward propagation of the AO signature and realistic seasonal evolution of lag correlations (as in Figure 5) have been observed in the UKMO Unified model (P. McCloghrie, Oxford University, personal communication).

The mechanism for downward propagation of AO anomalies likely involves modulation of the waveguide for planetary-scale waves by high-altitude anomalies. In zonal-mean wind, anomalies modify the climatological waveguide and distribution of acceleration from convergence of the Eliassen-Palm flux [*Kodera et al.*, 1990]. The net result from an anomaly in the middle stratosphere appears to be that the zonal-mean wind below the anomaly, over a period of days, tends to follow the anomaly above. This process may be difficult to observe because the downward propagation involves low-frequency anomalies and not day-to-day variability. An understanding of the mechanism involved will likely require experiments with mechanistic and climate models. Such experiments may illuminate what is required of medium-range weather forecasting models to exploit stratospheric variability to improve weather forecasts. The variable time for stratospheric anomalies to penetrate the troposphere may be an indication that the tropospheric anomalies may be largely independent of the stratosphere until they are of the same sign. In this case, the appearance of downward propagation would be the result of amplification of the AO anomalies when they align in the vertical. Nearly every instance of a large-amplitude tropospheric anomaly shows a strong connection to the stratosphere, suggesting that tropospheric variability would be less without influence from the stratosphere.

The pattern correlation of SLP and lower stratospheric geopotential is greater than that between SLP and midtropospheric geopotential (Figure 1). Thompson and Wallace suggested that the midtropospheric pattern is a hydrostatic response to low-level thermal advection attributable to winds associated with the SLP pattern. The vertically averaged temperature advection calculated by *Thompson and Wallace* [1999] is entirely consistent with this interpretation. It is therefore important to understand the cause of the SLP anomaly and its relation to the precursor signal in the upper troposphere and lower stratosphere. Elevation of polar-cap SLP implies a net transport of mass into this region and vice versa. A possible mechanism for the influx of mass is an anomalous westward (negative) body force in the upper troposphere or lower stratosphere in middle to high latitudes. The Eulerian mean meridional circulation induced by such a force is generally poleward and downward, tending to counteract the applied force, with an equatorward return flow in the lowermost troposphere. *Haynes and Shepherd* [1989] noted that streamlines of induced mean meridional circulation are not completely closed, because of the proximity of lower boundary. The low-level return flow therefore does not entirely cancel the transport of mass in the upper branch, and, as a result, surface pressure in the polar cap increases. This mechanism is linear, and the argument may be applied, in reverse, for a positive body force anomaly.

It is possible that an AO anomaly, equivalent barotropic in the vertical, creates conditions favorable for maintenance of the anomaly by modifying the direction of eddy momentum transport and wave breaking in the upper troposphere and lower stratosphere [*Thorncroft et al.*, 1993]. The role of eddy forcing remains to be demonstrated, and (if important) the relative contribution of synoptic and planetary-scale waves should be evaluated. Synoptic-scale waves are primarily important in the upper troposphere throughout the year, while planetary waves are primarily important in the stratosphere during winter when winds are westerly [*Charney and Drazin*, 1961]. It appears that planetary waves play an important, though indirect, role in causing the large-amplitude stratospheric AO anomalies which propagate slowly downward to affect the troposphere. It is possible that a positive feedback mechanism is involved. These considerations invite questions for further study. Is the stratospheric forcing directly responsible for evolution of the tropospheric AO anomaly in winter, or is its influence indirect, triggering a modification of transport by synoptic waves? Is the influence of stratospheric forcing felt primarily on timescales longer than a month? Our analysis of lag correlations suggests that the downward propagation through the troposphere of a "clean" AO signal is observed in low-pass-filtered data but not in unfiltered data. This result may be attributable to high-frequency fluctuations associated with tropospheric weather systems and to modification of the zonal-mean wind profile affecting the vertical propagation of planetary waves into the lower stratosphere on timescales shorter than a month.

5. Glossary

AO index: The principal component time series of the first EOF of 90-day low-pass filtered December-February geopotential at five levels (1000, 300, 100, 30, 10 hPa).

AO signature: Regression of the AO index with a data field, such as zonal-mean wind or geopotential at one of 17 pressure levels.

AO signature time series: The daily value of the AO signature defined by the multiple of the AO signature, α, that results in a "best fit" to the data. For each of 17 levels there is a 40-year time series.

Climatological AO amplitude: The rms value of the AO signature time series, which varies by day of year and level.

Acknowledgments. This research was supported by the National Science Foundation, grants ATM-9500613 and ATM-9708026, and by the National Aeronautics and Space Administration, contract NAS1-96071. The NCEP Reanalysis data were provided by the NOAA-CIRES Climate Diagnostics Center, Boulder, Colorado, from their Web site at http://www.cdc.noaa.gov. We thank the following people for helpful discussions: M. Allen, R. Black, N. Gillett, L.J. Gray, P.H. Haynes, W.A. Lahoz, P. McCloghrie, M.E. McIntyre, W.A. Norton, A. O'Neill, D.W.J. Thompson and J.M. Wallace.

References

Baldwin, M.P., and T.J. Dunkerton, Quasi-biennial modulation of the southern hemisphere stratospheric polar vortex, *Geophys. Res. Lett., 25*, 3343–3346, 1998.

Baldwin, M.P., X. Cheng, and T.J. Dunkerton, Observed correlations between winter-mean tropospheric and stratospheric circulation anomalies, *Geophys. Res. Lett., 21*, 1141–1144, 1994.

Bretherton, C.S., C. Smith, and J.M. Wallace, An intercomparison of methods for finding coupled patterns in climate data, *J. Clim., 5*, 541–560, 1992.

Charney, J.G., and P.G. Drazin, Propagation of planetary-scale disturbances from the lower into the upper atmosphere, *J. Geophys. Res., 66*, 83–109, 1961.

Dunkerton, T.J., and M.P. Baldwin, Modes of variability in the stratosphere, *Geophys. Res. Lett., 19*, 49–52, 1992.

Haynes, P.H., and T.G. Shepherd, The importance of surface pressure changes in the response of the atmosphere to zonally symmetric thermal and mechanical forcing, *Q. J. R. Meteorol. Soc., 115*, 1181–1208, 1989.

Holton, J.R., and H.-C. Tan, The influence of the equatorial quasi-biennial oscillation on the global circulation at 50 mb, *J. Atmos. Sci., 37*, 2200–2208, 1980.

Hurrell, J.W., Decadal trends in the North Atlantic Oscillation: Regional temperatures and precipitation, *Science, 269*, 676–679, 1995.

Kalnay, M.E., et al., The NCEP/NCAR Reanalysis Project, *Bull. Am. Meteorol. Soc., 77*, 437–471, 1996.

Kerr, R., A new force in high-latitude climate, *Science, 284*, 241–242, 1999.

Kodera, K., and H. Koide, Spatial and seasonal characteristics of recent decadal trends in the northern hemispheric troposphere and stratosphere, *J. Geophys. Res., 102*, 19,433–19,447, 1997.

Kodera, K., K. Yamazaki, M. Chiba, and K. Shibata, Downward propagation of upper stratospheric mean zonal wind perturbation to the troposphere, *Geophys. Res. Lett., 17*, 1263-1266, 1990.

Kodera, K., H. Koide, and H. Yoshimura, Northern hemisphere winter circulation associated with the North Atlantic Oscillation and stratospheric polar night jet, *Geophys. Res. Lett., 26*, 443–446, 1999.

Kutzbach, J.E., Large-scale features of monthly mean northern hemisphere anomaly maps of sea-level pressure, *Mon. Weather Rev., 98*, 708–716, 1970.

Nigam, S., On the structure of variability of the observed tropospheric and stratospheric zonal-mean wind, *J. Atmos. Sci., 47*, 1799–1813, 1990.

Quiroz, R.S., The association of stratospheric warmings with tropospheric blocking, *J. Geophys. Res., 91*, 5277–5285, 1986.

Shindell, D.T., R.L. Mille, G. Schmidt, and L. Pandolfo, Simulation of recent northern winter climate trends by greenhouse-gas forcing, *Nature, 399*, 452–455, 1999.

Thompson, D.W.J., and J.M. Wallace, The Arctic Oscillation signature in the wintertime geopotential height and temperature fields, *Geophys. Res. Lett.*, 25, 1297–1300, 1998.

Thompson, D.W.J., and J.M. Wallace, The structure of the Arctic and Antarctic oscillations, *J. Climate*, in press, 1999.

Thorncroft, C.D., B.J. Hoskins and M.E. McIntyre, Two paradigms of baroclinic-wave life-cycle behaviour. *Q. J. R. Meteorol. Soc., 119*, 17–56, 1993.

Walker, G.T., and E.W. Bliss, World Weather V, *Mem. R. Meteorol. Soc., IV, 36*, 1932.

M.P. Baldwin and T.J. Dunkerton, Northwest Research Associates, 14508 NE 20th Street, Bellevue, WA 98007-3713. (mark@nwra.com, tim@nwra.com)

(Received January 28, 1999; revised April 28, 1999; accepted June 17, 1999.)